

Iron Availability Influences Silicon Isotope Fractionation  
in Two Southern Ocean Diatoms (*Proboscia inermis*  
and *Eucampia antarctica*) and a Coastal Diatom  
(*Thalassiosira pseudonana*)



# Iron Availability Influences Silicon Isotope Fractionation in Two Southern Ocean Diatoms (*Proboscia inermis* and *Eucampia antarctica*) and a Coastal Diatom (*Thalassiosira pseudonana*)

Scott Meyerink<sup>1\*</sup>, Michael J. Ellwood<sup>1\*</sup>, William A. Maher<sup>2</sup> and Robert Strzepek<sup>1</sup>

<sup>1</sup> Research School of Earth Sciences, Australian National University, Canberra, ACT, Australia

<sup>2</sup> Ecochemistry Laboratory, Institute for Applied Ecology, University of Canberra, Canberra, ACT, Australia

**Edited by:**

Brivaela Moriceau, Centre National de la Recherche Scientifique, France

**Reviewed by:**

Damien Cardinal, Université Pierre et Marie Curie, France

Frank Dehairs, Vrije Universiteit Brussel, Belgium

\* **Correspondence:** Scott Meyerink, [scott.meyerink@anu.edu.au](mailto:scott.meyerink@anu.edu.au)

Michael J. Ellwood, [michael.ellwood@anu.edu.au](mailto:michael.ellwood@anu.edu.au)

**Specialty section:** This article was submitted to Marine Biogeochemistry, a section of the journal *Frontiers in Marine Science*

**Received:** 28 February 2017

**Accepted:** 22 June 2017

**Published:** 07 July 2017

**Citation:** Meyerink S, Ellwood MJ, Maher WA and Strzepek R (2017) Iron Availability Influences Silicon Isotope Fractionation in Two Southern Ocean Diatoms (*Proboscia inermis* and *Eucampia antarctica*) and a Coastal Diatom (*Thalassiosira pseudonana*). *Front. Mar. Sci.* 4:217. doi: 10.3389/fmars.2017.00217

The fractionation of silicon (Si) isotopes was measured in two Southern Ocean diatoms (*Proboscia inermis* and *Eucampia Antarctica*) and a coastal diatom (*Thalassiosira pseudonana*) that were grown under varying iron (Fe) concentrations. Varying Fe concentrations had no effect on the Si isotope enrichment factor ( $\epsilon$ ) in *T. pseudonana*, whilst *E. Antarctica* and *P. inermis* exhibited significant variations in the value of  $\epsilon$  between Fe-replete and Fe-limited conditions. Mean  $\epsilon$  values in *P. inermis* and *E. Antarctica* decreased from ( $\pm$  1SD)  $-1.11 \pm 0.15\text{‰}$  and  $-1.42 \pm 0.41 \text{‰}$  (respectively) under Fe-replete conditions, to  $-1.38 \pm 0.27 \text{‰}$  and  $-1.57 \pm 0.5 \text{‰}$  (respectively) under Fe-limiting conditions. These variations likely arise from adaptations in diatoms arising from the nutrient status of their environment. *T. pseudonana* is a coastal clone typically accustomed to low Si but high Fe conditions whereas *E. Antarctica* and *P. inermis* are typically accustomed to High Si, High nitrate low Fe conditions. Growth induced variations in silicic acid ( $\text{Si}(\text{OH})_4$ ) uptake arising from Fe-limitation is the likely mechanism leading to Si-isotope variability in *E. Antarctica* and *P. inermis*. The multiplicative effects of species diversity and resource limitation (e.g., Fe) on Si-

isotope fractionation in diatoms can potentially alter the Si-isotope composition of diatom opal in diatomaceous sediments and sea surface Si(OH)<sub>4</sub>. This work highlights the need for further *in vitro* studies into intracellular mechanisms involved in Si(OH)<sub>4</sub> uptake, and the associated pathways for Si-isotope fractionation in diatoms.

**Keywords: silicon isotopes, Southern Ocean, diatom, isotope fractionation, iron**

## INTRODUCTION

Diatoms play a vital role in the biogeochemical cycles of carbon (C) and silicon (Si). They dominate the production of biogenic silica (BSi) in the ocean, and hence have a controlling influence on the marine Si cycle through the utilization of dissolved silicon [silicic acid, Si(OH)<sub>4</sub>], which they use in the formation of their cell wall, or frustule (Nelson et al., 1995; Tréguer et al., 1995; Tréguer and De La Rocha, 2013). Diatoms make up a significant proportion of phytoplankton communities in nutrient rich regions of the ocean such as the Southern Ocean, where they contribute significantly to the deep export of C and Si to ocean sediments (Smetacek, 1999; Kemp et al., 2000; Roca-Martí et al., 2017). BSi preservation rates can reach as high as 30% in some of these areas due to increased sedimentation rates of diatom produced opaline silica (McManus et al., 1995; Nelson et al., 1995; Ragueneau et al., 2000). While the accumulation of sedimentary BSi (or opal) presents a promising tool for reconstructing the degree of coupling between the Si and C cycles, indices based on the accumulation of sedimentary opal are often subject to winnowing and focusing of sediments, and the dissolution of opal at the sediment-water interface (De La Rocha et al., 1998; Ragueneau et al., 2000). Variations in the ratios of <sup>30</sup>Si to <sup>28</sup>Si (expressed as δ<sup>30</sup>Si in ‰) in opaline sediments and in the Si(OH)<sub>4</sub> pool present in surface waters represents a promising tool in providing information on the marine Si cycle, and as such, has been used as a proxy for marine diatom production and Si(OH)<sub>4</sub> utilization in several palaeo-oceanographic studies (De La Rocha et al., 1998; Beucher et al., 2007; Pichevin et al., 2009; Ellwood et al., 2010; Rousseau et al., 2016); and in field studies (Varela et al., 2004; Cardinal et al., 2007; Beucher et al., 2011).

During Si uptake, diatoms discriminate against heavier isotopes, which changes the isotopic composition of both the diatom opal and the residual Si(OH)<sub>4</sub> pool (De La Rocha et al., 1997; Sutton et al., 2013). This results in a lighter isotope composition (<sup>28</sup>Si or <sup>29</sup>Si vs. <sup>30</sup>Si) in the frustule, relative to its dissolved Si source. Although the exact mechanism of fractionation of silicon isotopes in diatoms is unknown, fractionation has been determined to resemble Rayleigh style fractionation kinetics under closed-system conditions, where the substrate [dissolved Si in the form of Si(OH)<sub>4</sub>] is precipitated into the product, BSi (Criss and Criss, 1999). The isotope fractionation factor (α) for Rayleigh fractionation determines the rate of fractionation between the Si(OH)<sub>4</sub> and the Si-BSi product, and is calculated by the following equation (De La Rocha et al., 1997):

$$\alpha_{BSi-DSi} = \frac{\ln\left(1 - \left(\frac{(1+\delta^{30}Si_{acc}/1000)(1-f)}{(1+\delta^{30}Si_o/1000)}\right)\right)}{\ln f} \quad (1)$$

where α<sub>BSi—DSi</sub> is the isotope fractionation factor between the Si(OH)<sub>4</sub> and the BSi product, *f* is the fractional depletion of Si(OH)<sub>4</sub> in the media and δ<sup>30</sup>Si<sub>acc</sub> and δ<sup>30</sup>Si<sub>o</sub> are the δ<sup>30</sup>Si values of the

accumulated BSi and of  $\text{Si}(\text{OH})_4$  in the media at  $f = 1.0$  (respectively). Isotope fractionation is often described in terms of a per mil (‰) value such as the enrichment factor ( $\epsilon$ ). The relationship between  $\alpha$  and  $\epsilon$  can be described using the following equation:

$$\epsilon(\text{‰}) = (\alpha - 1) \times 1000 \quad (2)$$

Estimates for Si isotope fractionation in diatoms under controlled laboratory conditions were initially found to be (expressed as  $\epsilon$  in ‰),  $-1.1 \pm 0.4$  ‰ (average  $\pm$  1SD), with little variation between species (*Thalassiosira* sp., *Thalassiosira weissflogii* and *Skeletonema costatum*) (De La Rocha et al., 1997). Fractionation was also found to be independent of changes in temperature (12–22°C) (De La Rocha et al., 1997); Si quota, Si efflux and  $p\text{CO}_2$  concentration in *T. weissflogii* (Milligan et al., 2004). While these studies focused mainly on temperate and sub-polar species of diatoms, they did not adequately represent the isotope composition of individual Polar and Southern Ocean diatoms, and further studies found an inter-species effect between the Southern Ocean diatoms *Fragilariopsis kergulensis* ( $-0.54 \pm 0.09$  ‰) and *Chaetoceros brevis* ( $-2.09 \pm 0.09$  ‰) (Sutton et al., 2013). While the reasons for the difference in isotopic composition of these species is unclear, Sutton et al. (2013) suggested that potential phylogenetic and morphological effects could play an important role in Si isotope fractionation.

Diatoms in the Southern Ocean experience rapid fluctuations in both physical and chemical conditions associated with the variations in sea ice extent, deep winter mixing and alterations in nutrient supply (Sackett et al., 2013). In the short term, these extremes in physico-chemical conditions can potentially influence Si isotope fractionation in diatoms through variations in cell morphology, growth rate and nutrient uptake rate (Hutchins and Bruland, 1998; Takeda, 1998; Brzezinski et al., 2002; Leynaert et al., 2004; Meyerink et al., 2017). Field studies show that Si isotopic fractionation by siliceous phytoplankton varies across the Antarctic Polar Frontal Zone (APFZ), and coincides with the presence of a strong northward gradient in  $\text{Si}(\text{OH})_4$  concentrations (Cardinal et al., 2007; Fripiat et al., 2011). Despite the large zonal variations in Si isotopic fractionation, there was no change among different size fractions, suggesting that the latitudinal variations in Si isotope fractionation in siliceous phytoplankton could be a direct result of nutrient availability, more than species composition (Cardinal et al., 2007). In order to decipher the effects both factors have on the surface Si isotope composition in the Southern Ocean, a better understanding of the effects nutrient availability has on Si isotope fractionation in diatoms is required.

Iron (Fe) availability affects the growth rate, Si uptake, cell morphology and BSi content in diatoms (Leynaert et al., 2004; Hoffmann et al., 2008; Marchetti and Cassar, 2009; Boutorh et al., 2016; Meyerink et al., 2017). These microscale effects can have far reaching consequences on the physico-chemical environment, particularly in the Southern Ocean. Fe-limited diatoms in Antarctic water take up more  $\text{Si}(\text{OH})_4$  relative to nitrate ( $\text{NO}_3^-$ ), so that by the time surface waters reach the sub-Antarctic zone (SAZ), it is depleted in  $\text{Si}(\text{OH})_4$  relative to  $\text{NO}_3^-$  (Varela et al., 2004; Matsumoto et al., 2014). Alleviation of Fe-limitation in Antarctic waters may have potentially altered the  $\text{Si}(\text{OH})_4$ : $\text{NO}_3^-$  uptake ratio in diatoms during glacial times, and resulted in a “leakage” of silicic acid to sub-polar waters (Brzezinski et al., 2002; Matsumoto et al., 2002). Opaline sediments exhibit variations in their Si isotope composition from glacial times, and can potentially be a useful tool in resolving the mechanisms behind the glacial-interglacial transitions of the past (De La Rocha et al., 1998; Beucher et al., 2007; Pichevin et al., 2009; Ellwood et al., 2010; Rousseau et al., 2016). In order to

quantitatively use  $\delta^{30}\text{Si}$  to determine diatom production during these periods, a better understanding of how Fe-availability affects diatom  $\delta^{30}\text{Si}$  composition is required; especially since it is thought that the supply of Fe to Southern Ocean waters was higher during glacial periods (Martinez-Garcia et al., 2011). Here, the results of the fractionation of Si-isotopes in these diatoms under varying degrees of Fe-limitation are presented.

## METHODS

### Culture Conditions

The centric diatom *T. pseudonana* (Strain CS-20) was obtained from the Australian national algae culture collection in Hobart, Australia and maintained in *f/2* medium (CSIRO recipe) at 20°C under a continuous photon flux density (PFD) of 120–145  $\mu\text{E m}^{-2} \text{s}^{-1}$ , before being transferred to Fe-replete Aquil medium (Price et al., 1988). Stock cultures of the Southern Ocean diatoms *P. inermis* and *E. Antarctica* were isolated from waters south of the Antarctic Polar Frontal Zone in December 2001 (Strzepek et al., 2011). The Southern Ocean diatoms have since been maintained in Fe-replete Aquil medium at a temperature of 3°C under a continuous photon flux density (PFD) of  $\sim 35 \mu\text{E m}^{-2} \text{s}^{-1}$ . Cultures were acclimated to the different Fe concentrations in 28 mL polycarbonate vials for a minimum of three transfers (approximately 10–12 generations), before being transferred to 1 L polycarbonate bottles for experimental work. All cultures were grown in batches rather than under semi-continuous conditions to minimize contamination from trace metals. Average PFD's for cultures of *E. Antarctica*, *P. inermis*, and *T. pseudonana* were 45  $\mu\text{E m}^{-2} \text{s}^{-1}$ , 60  $\mu\text{E m}^{-2} \text{s}^{-1}$  and 133  $\mu\text{E m}^{-2} \text{s}^{-1}$  respectively (Sunda and Huntsman, 1997; Strzepek et al., 2012). Experimental temperatures were 20°C for *T. pseudonana* and 3°C for the Southern Ocean species.

### Medium Preparation

Aquil medium was prepared using trace-metal ultra-clean techniques and enriched with the following nutrients; 10  $\mu\text{mol L}^{-1}$  phosphate, 100  $\mu\text{mol L}^{-1}$   $\text{Si}(\text{OH})_4$ , 300  $\mu\text{mol L}^{-1}$  nitrate, 0.55  $\mu\text{g L}^{-1}$  vitamin  $\text{B}_{12}$ , 0.5  $\mu\text{g L}^{-1}$  Biotin and 100  $\mu\text{g L}^{-1}$  thiamin. Basal medium and stock solutions were eluted through a column containing Toyopearl AF-chelate-650M (Tosohbioscience) ion-exchange resin to remove metal contaminants and filter sterilized (0.2  $\mu\text{m}$ ) (Price et al., 1988). Iron contamination of the basal medium was measured using high-resolution IC-PMS after pre-concentration (Ellwood et al., 2008) and found to be  $0.56 \pm 0.02 \text{ nmol L}^{-1}$  ( $n = 3$ ). Trace metal ion concentrations were controlled through the addition of a trace-metal ion buffer system, which used 10 and 100  $\mu\text{mol L}^{-1}$  ethylene-diamine-tetra-acetic-acid (EDTA), as the chelating agent, for both Southern Ocean species and *T. pseudonana* (respectively). Trace metal concentrations were 7.91  $\text{nmol L}^{-1}$   $\text{ZnSO}_4$ , 1.98  $\text{nmol L}^{-1}$   $\text{CuSO}_4$ , 5  $\text{nmol L}^{-1}$   $\text{CoCl}_2$ , 22.8  $\text{nmol L}^{-1}$   $\text{MnCl}_2$ , 9.96  $\text{nmol L}^{-1}$   $\text{Na}_2\text{SeO}_3$  and 100  $\text{nmol L}^{-1}$   $\text{Na}_2\text{MoO}_4$  for media containing *P. inermis* and *E. Antarctica*; and 100  $\text{nmol L}^{-1}$   $\text{ZnSO}_4$ , 40  $\text{nmol L}^{-1}$   $\text{CuSO}_4$ , 40  $\text{nmol L}^{-1}$   $\text{CoCl}_2$ , 100  $\text{nmol L}^{-1}$   $\text{MnCl}_2$ , 10  $\text{nmol L}^{-1}$   $\text{Na}_2\text{SeO}_3$  and 100  $\text{nmol L}^{-1}$   $\text{Na}_2\text{MoO}_4$  for media containing *T. pseudonana*. Free ion concentrations were calculated using Visual MINTEQ, giving concentrations (expressed as  $-\log$  free metal ion concentration =  $p\text{Metal}$ ) of,  $p\text{Cu}$  14.07,  $p\text{Mn}$  8.18,  $p\text{Zn}$  10.78 and  $p\text{Co}$  11.09 for Aquil medium at a temperature of 3°C and a pH of 8.4 for Southern Ocean media,

while *pMetal* values for *T. pseudonana* media were *pCu* 13.65, *pMn* 8.35, *pZn* 10.72 and *pCo* 11.26 for Aquil medium at a temperature of 20°C and a pH of 8.1.

## Measurement of Culture pH

Culture pH was measured by the change in absorbance of m-cresol purple in culture medium at specific wavelengths of 434, 578, and 730 nm respectively on a Varian Cary 1E UV-visible spectrophotometer with attached temperature controller (Clayton and Byrne, 1993; Yao et al., 2007). Measurements were made at 25°C and corrected for dye-induced changes in the pH. The pH was then adjusted to the culture temperature of 20°C using CO2SYS (<http://cdiac.ornl.gov/oceans/co2rpert.html>).

## Iron Manipulation

*T. pseudonana* cultures were treated with a range of Fe concentrations varying from Fe limiting to Fe replete: from 30 through to 50, 80, 250, and 500 nmol L<sup>-1</sup> of total dissolved Fe, equating to -log Fe<sup>3+</sup> concentration (*pFe*) values of 20.59, 20.36, 20.16, 19.67, and 19.36 respectively. The Fe concentrations were selected to induce different degrees of limitation as defined by the reduction in growth rate from  $\mu_{max}$ . Inorganic Fe concentrations (Fe') were calculated according to Sunda and Huntsman (2003) for a temperature of 20°C, a mean irradiance of 133  $\mu E m^{-2} s^{-1}$  and a mean starting pH of 7.98. Fe' values based on total dissolved Fe concentrations of 500, 250, 80, 50, and 30 nM equated to 0.42, 0.21, 0.07, 0.04, and 0.02 nM respectively (Table 1) (Sunda and Huntsman, 2003).

**Table 1.** Culture conditions, growth rates, Fe concentrations and Results from the Si isotope fractionation experiments for *Proboscia inermis*, *Eucampia antarctica* and *Thalassiosira pseudonana*.

Fe treatment	Fe' (pmol L <sup>-1</sup> )	Number of replicate cultures	$\mu$ (d <sup>-1</sup> )	PFD ( $\mu E m^{-2} s^{-1}$ )	<i>n</i>	$\delta^{30}Si_{NBS28}$ (per mil)	<i>f</i>	$\alpha$	Fractionation factor ( $\epsilon$ , ‰)	<i>P</i>
<b><i>P. inermis</i></b>										
58.3 nmol L <sup>-1</sup> Fe; 10 $\mu$ mol L <sup>-1</sup> EDTA	3369	3	0.35 ± 0.02	60	9	-0.55 ± 0.16	0.97 ± 0.06	0.9989 ± 0.0002	-1.11 ± 0.15	
4.4 nmol L <sup>-1</sup> Fe; 80 nmol L <sup>-1</sup> DFB	0.09	2	0.09 ± 0.02	60	5	-0.6 ± 0.23	0.68 ± 0.06	0.9986 ± 0.0003	-1.38 ± 0.27	0.08
<b><i>E. antarctica</i></b>										
58.3 nmol L <sup>-1</sup> Fe; 10 $\mu$ mol L <sup>-1</sup> EDTA	3369	4	0.32 ± 0.02	50	12	-0.65 ± 0.33	0.7 ± 0.02	0.9986 ± 0.0004	-1.42 ± 0.41	
4.4 nmol L <sup>-1</sup> Fe; 40 nmol L <sup>-1</sup> DFB	0.2	4	0.07 ± 0.01	50	11	-0.8 ± 0.48	0.72 ± 0.07	0.9984 ± 0.0005	-1.57 ± 0.5	0.04
<b><i>T. pseudonana</i></b>										
500 nmol L <sup>-1</sup> Fe; 100 $\mu$ mol L <sup>-1</sup> EDTA	418	1	1.52*	133	3	0.09 ± 0.08	0.60	0.9994 ± 0.0001	-0.59 ± 0.11	
250 nmol L <sup>-1</sup> Fe; 100 $\mu$ mol L <sup>-1</sup> EDTA	208	1	1.48*	133	3	0.13 ± 0.37	0.65	0.9995 ± 0.0005	-0.51 ± 0.46	0.8
80 nmol L <sup>-1</sup> Fe; 100 $\mu$ mol L <sup>-1</sup> EDTA	67	1	0.85*	133	3	0.13 ± 0.08	0.67	0.9995 ± 0.0001	-0.51 ± 0.1	0.39
30 nmol L <sup>-1</sup> Fe; 100 $\mu$ mol L <sup>-1</sup> EDTA	25	2	0.72 ± 0.01	133	6	-0.07 ± 0.08	0.87 ± 0.01	0.9993 ± 0.0001	-0.65 ± 0.08	0.42
Growth Media Si (Aquil replicates)					6	0.54 ± 0.13				
Growth Media Si (NaOH replicates)					3	0.53 ± 0.02				
Mean Growth Media Si (Aquil + NaOH replicates)					9	0.54 ± 0.11				

Fractionation factors were calculated from diatom silica as a function of *f*, where *f* is the fraction of the original Si(OH)<sub>4</sub> remaining in the system once diatoms were harvested. *n* is the number of measurements from cultures. All values presented as means ± 1 SD. *P*-values are relative to Fe-replete (Fe+) conditions. For *T. pseudonana*, the Fe-replete concentration is equal to an Fe' value of 418 pmol L<sup>-1</sup>.

\*Maximum growth rate from single replicate culture. Because there was no difference in  $\epsilon$  between replicate cultures, the value for  $\epsilon$  is the mean of all cultures ± 1 SD.

Southern Ocean cultures were treated differently to *T. pseudonana* cultures, and two competing ligands were used to induce Fe-limitation. This is because Southern Ocean diatoms are well adapted

to iron limiting conditions over coastal isolates such as *T. pseudonana*. Iron replete media was prepared through the addition of a filter-sterilized FeEDTA complex (1:1.05[mol:mol]) to Aquil containing  $10 \mu\text{mol L}^{-1}$  EDTA for a final concentration (including contamination) of  $58.3 \text{ nmol L}^{-1}$  of total dissolved Fe. Iron limited media was prepared by adding Fe pre-complexed with the terrestrial siderophore desferrioxamine B mesylate (DFB; Sigma Aldridge) to Aquil media containing  $10 \mu\text{mol L}^{-1}$  EDTA for a final concentration of  $4.4 \text{ nmol L}^{-1}$ . Varying degrees of Fe limitation were induced in culture by increasing the amount of DFB in culture at concentrations of 40 and  $80 \text{ nmol L}^{-1}$  for *E. Antarctica* and *P. inermis* (respectively). The Fe' concentration in the iron-replete media was calculated according to Sunda and Huntsman (2003) for a temperature of  $3^\circ\text{C}$ , a mean irradiance of  $52 \mu\text{E m}^{-2} \text{ s}^{-1}$  and a pH of 8.4. The overall conditional dissociation constant ( $K'_a$ ) was calculated according to methods described by Strzepek et al. (2011) and represents the sum of the conditional stability constant in the dark ( $3.52 \times 10^{-7}$ ) and the conditional photo-dissociation constant ( $K_{\text{hv}} = 2.17 \times 10^{-6}$ ) of EDTA at  $3^\circ\text{C}$ . The Fe' concentration for FeDFB treatment was calculated according to the equation  $[\text{Fe}'] = [\text{FeDFB}] / [\text{L}'] \times K_{\text{Fe}'\text{L}}^{\text{cond}}$ ; where  $K_{\text{Fe}'\text{L}}^{\text{cond}} = 10^{11.8}$  (Maldonado et al., 2005). In the instance where total Fe exceeded the concentration of DFB bound Fe ( $\text{Fe}_{\text{tot}} = 4.4 \text{ nmol L}^{-1}$ ;  $\text{DFB} = 4 \text{ nmol L}^{-1}$ ), we assumed a  $0.1 \text{ nmol L}^{-1}$  excess of DFB in the media and a  $0.5 \text{ nmol L}^{-1}$  excess of total Fe that was available for interaction with EDTA (Table 1).

### **Specific Growth Rate, Cell Counts and $\text{Si}(\text{OH})_4$ Consumption**

Growth rates were determined from *in vivo* chlorophyll *a* fluorescence using a Turner Designs model 10-AU Fluorometer. Specific growth rates of exponentially growing cultures were determined from linear regressions of  $\ln$  *in vivo* fluorescence vs. time. Cell density ( $\text{cells mL}^{-1}$ ) was determined by microscopy (Sedgewick-Rafter or Haemocytometer – brightline, Neubauer improved). Each sample was enumerated a minimum of three times resulting in a S.E between counts  $<11\%$  for *P. inermis* and *E. Antarctica*, and  $<5\%$  for *T. pseudonana*. Consumption of  $\text{Si}(\text{OH})_4$  in culture was obtained by measuring samples of culture media shortly after inoculation and at the exponential stage of growth (respectively), when cultures were harvested.

### **$\delta^{30}\text{Si}$ Determination of Diatom Silica**

Once cultures were in their exponential phase of growth, 50–100 ml of cell culture was collected onto a  $2 \mu\text{m}$ , 25 mm polycarbonate filter, rinsed with nutrient free Aquil, and washed into 3 mL Teflon bombs. Purification of the samples were done according to similar methods for sponge spicules by Wille et al. (2010). The samples were evaporated to dryness at  $50^\circ\text{C}$  in a drying oven overnight. To remove organics, samples were treated with 1 mL of 30% hydrogen-peroxide ( $\text{H}_2\text{O}_2$ ) solution, and allowed to reflux for 24 h at  $70^\circ\text{C}$  on a hotplate. Following oxidation, the lids were removed, and the samples were left to evaporate to dryness before adding 2 ml of 0.5 M sodium hydroxide (NaOH) to dissolve the sediment. Samples were then left to reflux overnight again for 24 h at  $50^\circ\text{C}$ . The  $\text{Si}(\text{OH})_4$  concentration within the sample digest was then measured colorimetrically (Strickland and Parsons, 1965). Sodium was removed from the samples using cation exchange columns to prevent any subsequent interference during isotope determination. Cation exchange columns consisted on 1 mL Dowex 50W-X8 cation exchange resin (200–400 mesh) with a 2.5 mL reservoir. Columns were cleaned with 0.5 mL 8% (w/w) hydrofluoric acid (HF) followed by 2.25 mL of deionized water. The

resin with protonated by passing 2.25 mL of 4 mol L<sup>-1</sup> HCl followed by 2.25 mL of deionized water. The columns were then loaded with 0.5 mL of sample, before being rinsed with 4 × 0.5 mL of deionized water. To minimize contamination, samples were collected in vials that were cleaned using 8% (w/w) HF, before being rinsed with deionized water. Samples for δ<sup>30</sup>Si determination of the growth media were prepared by dissolving the sodium silicate standard used for nutrient enrichment in the growth medium to a concentration of 2 mmol L<sup>-1</sup> in separate solutions of nutrient free Aquil and 0.5 M sodium hydroxide. These samples were then treated with the same column procedure as the cell samples prior to analysis.

## Determination of δ<sup>30</sup>Si of Diatom Silica

The δ<sup>30</sup>Si composition of diatom silica was determined according to methods developed by Wille et al. (2010) using a multi-collector inductively coupled plasma mass spectrometer (MC-ICP-MS) (Finnigan Neptune, Germany) operating in dry plasma mode at medium-resolution (M/ΔM ~2,000). An ESI-Apex nebulizer fitted with a Teflon inlet system and a demountable torch fitted with an alumina injector was used for sample introduction to minimize any background interference. A standard-sample-standard bracketing technique was used for data acquisition and reduction (Wille et al., 2010). The δ<sup>30</sup>Si signal (based on the relative abundance of <sup>30</sup>Si to <sup>28</sup>Si (<sup>30</sup>Si/<sup>28</sup>Si)) was calculated using the following formula:

$$\delta^{30}\text{Si} = \left[ \left( \frac{R_{\text{Sample}}}{R_{\text{Std}}} \right) - 1 \right] \times 1000 \quad (3)$$

Where  $R_{\text{sample}}$  is the ratio of <sup>30</sup>Si/<sup>28</sup>Si of the sample and  $R_{\text{Std}}$  is the <sup>30</sup>Si/<sup>28</sup>Si of the in-house standard developed from dissolution a diatomaceous sediment and purified (Figure 1). Measurements of sample blanks were made prior to each run to ensure that the combined blank and background was <1% of the total sample signal. Inter-laboratory NBS-28 and diatomite standards were prepared with each daily run, and were measured with every three samples (≤ 8 diatomite/NBS -28 standards per daily run).

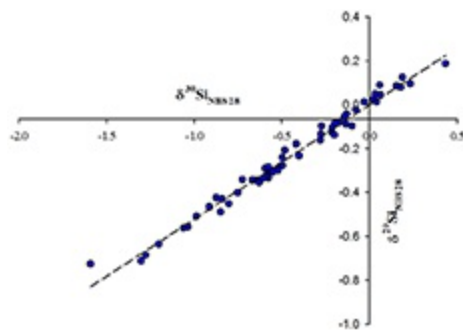


**FIGURE 1.** Mass dependent fractionation of δ<sup>29</sup>Si vs. δ<sup>30</sup>Si for all diatom samples relative to NBS-28. Regression line represents δ<sup>29</sup>Si = [0.520 ± 0.009]δ<sup>30</sup>Si - 0.002 ± 0.006, ( $r^2 = 0.99$ ,  $n = 55$  samples).

δ<sup>30</sup>Si and δ<sup>29</sup>Si values relative to NBS-28 plotted on an mass-dependent fractionation line with a slope of 0.520 ± 0.009 and is consistent with the consensus slope of 0.511 obtained from inter-laboratory silicon standard measurements (Reynolds et al., 2007). The reproducibility of the δ<sup>30</sup>Si signal measured for the NBS-28 standard (prepared in full and measured on 5 separate occasions)

was  $0.25 \pm 0.04$  ‰. Measurements of the “diatomite standard” produced a mean  $\delta^{30}\text{Si}$  value of  $1.29 \pm 0.25$  ‰ (2 SD,  $n = 33$ ), and is in good agreement with inter-laboratory comparisons ( $\delta^{30}\text{Si} = 1.27$  ‰) (Reynolds et al., 2007).

## RESULTS

Growth rates between replicate cultures varied by  $<6\%$  (coefficient of variation, CV) and  $f$  was kept above a value of 0.6 in all cultures (Table 1). All values for  $\epsilon$  are presented as means,  $\pm 1$  standard deviation (S.D.). *P. inermis*, *E. Antarctica* and *T. pseudonana* exhibited mean  $\epsilon$  values of  $-1.11 \pm 0.15$  ‰,  $-1.42 \pm 0.41$  ‰ and  $-0.59 \pm 0.11$  ‰, respectively when grown under Fe-replete conditions (Figure 2). The mean  $\epsilon$  values for *P. inermis* and *E. Antarctica* grown under Fe-replete conditions were not statistically different ( $p > 0.05$ ) from the mean value of  $-1.1$  ‰ obtained by De La Rocha et al. (1997); however, they were statistically different compared to the mean  $\epsilon$  value for *T. pseudonana* ( $p < 0.05$ ). Whilst a relatively low  $f$  compared to alternate studies (e.g., Sutton et al., 2013) may introduce an underestimation of the results (De La Rocha et al., 1997); the observation that *T. pseudonana* exhibited little variation in its isotope composition despite the range in  $f$  values suggests that this bias was insignificant (Table 2).

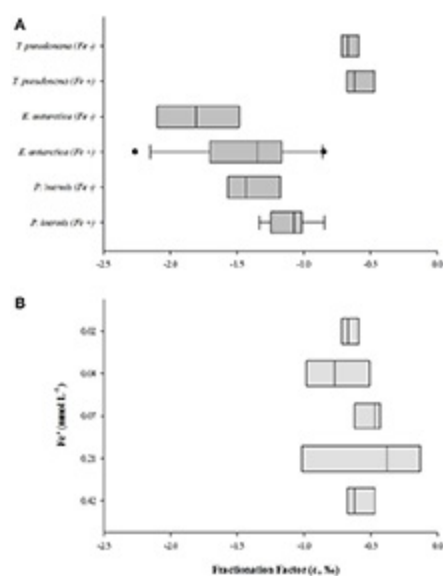


**FIGURE 2.** Box and whisker plot displaying the effects of Fe-availability on *T. pseudonana*, *P. inermis* and *E. Antarctica*. **(A)** Represents comparisons between all species, **(B)** represents the variation in Si-isotope fractionation factor across multiple Fe-concentrations for *T. pseudonana*. Lines are median values, Boxes represent 1st and 3rd quartiles and dots represent outliers ( $n \geq 3$ ).

**Table 2.** Comparison of Fe-replete, Si-isotope fractionation factors ( $\epsilon$ , ‰) between this study and previous studies.  $n$  is the number of replicate cultures.

Species name	Strain/Isolation source	PFD ( $\mu\text{E m}^{-2} \text{s}^{-1}$ )	$n$	Temperature (°C)	$\mu_{\text{max}}$ ( $\text{day}^{-1}$ )	$f$	Fractionation factor ( $\epsilon$ , ‰*)
<b>This study</b>							
<i>P. inermis</i>	ANARE V3 CLIVAR	60	3	3	0.35 ± 0.02	0.97 ± 0.06	-1.11 ± 0.15
<i>E. Antarctica</i>	ANARE V3 CLIVAR	50	4	3	0.32 ± 0.02	0.7 ± 0.02	-1.42 ± 0.41
<i>T. pseudonana</i> *	<b>CS-20</b>	<b>133</b>	<b>6</b>	<b>20</b>	<b>1.52*</b>	<b>0.77 ± 0.14</b>	<b>-0.61 ± 0.21</b>
Sutton et al., 2013							
<i>T. pseudonana</i>	<b>CCMP1014</b>	<b>200</b>	<b>4</b>	<b>18</b>	<b>1.30 ± 0.13</b>	<b>0.92 ± 0.005</b>	<b>-0.97 ± 0.14</b>
<i>T. pseudonana</i>	<b>CCCM58</b>	<b>200</b>	<b>4</b>	<b>18</b>	<b>1.34 ± 0.11</b>	<b>0.92 ± 0.007</b>	<b>-0.88 ± 0.06</b>
<i>T. weissflogii</i>	CCMP1010	200	3	18	0.66 ± 0.06	0.91 ± 0.15	-0.72 ± 0.04
<i>P. glacialis</i>	CCMP650	50	3	3	0.21 ± 0.01	0.91 ± 0.005	-1.15 ± 0.03
<i>F. kerguelensis</i>	LOHAFEX	90	4	3	0.22 ± 0.02	0.92 ± 0.007	-0.53 ± 0.11
<i>F. kerguelensis</i>	EIFEX	90	3	3	0.20 ± 0.02	0.9 ± 0.01	-0.56 ± 0.07
<i>T. antarctica</i>	CCMP982	30	3	3	0.19 ± 0.01	0.92 ± 0.001	-0.74 ± 0.05
<i>C. brevis</i>	CCMP164	90	4	3	0.36 ± 0.04	0.9 ± 0.01	-2.09 ± 0.09
<i>T. nordenskiöldii</i>	CCMP997	170	4	3	0.58 ± 0.01	0.92 ± 0.01	-1.21 ± 0.04
Milligan et al., 2004							
<i>T. weissflogii</i>	Coastal Strain	160	6	20	1.4 ± 0.05	0.88 ± 0.01	-1.58 ± 0.1
De La Rocha et al., 1997							
<i>S. costatum</i>	CCMP1332	99	4	15	No data reported	0.96 ± 0.03	-0.95 ± 0.4
<i>T. weissflogii</i>	Unknown source	99	4	15	No data reported	0.8 ± 0.08	-1.28 ± 0.46
<i>Thalassiosira</i> sp.	Isolate	99	5	15	No data reported	0.85 ± 0.03	-1.04 ± 0.42

All values presented as means ± 1 SD.  $\mu_{\text{max}}$  is the maximum growth rate per day. Inter-comparisons in  $\epsilon$  between *Thalassiosira pseudonana* strains in this study and previous studies by Sutton et al. (2013) are highlighted in bold. \*Maximum growth rate from single replicate culture. Because there was no difference in  $\epsilon$  between replicate cultures, the value for  $\epsilon$  is the mean of all cultures ± 1 SD.

## Effects of Fe-Availability on Si Isotope Fractionation

*T. pseudonana* displayed little variation in  $\epsilon$  with decreasing Fe concentration (Figure 2). No clear trends were observed across the five Fe-conditions, with  $\epsilon$  values ranging between  $0.51 \pm 0.46$  ‰ and  $0.75 \pm 0.24$  ‰. Comparisons of  $\epsilon$  values between Fe-limited ( $\text{Fe}' = 208, 67, 42, \text{ and } 25 \text{ pmol L}^{-1}$ ) and Fe-replete conditions ( $\text{Fe}' = 418 \text{ pmol L}^{-1}$ ) were not statistically significant (*ANOVA*,  $p > 0.1$ ). Because of the statistical insignificance between these  $\epsilon$  values, the mean was taken of all values ( $-0.61 \pm 0.21$  ‰) and compared against  $\epsilon$  values obtained from two strains of *T. pseudonana* (CCMP1014 and CCCM58,  $-0.97 \pm 0.14$  and  $-0.88 \pm 0.06$  ‰, respectively) cultured under Fe-replete conditions by Sutton et al. (2013). We observed a difference ( $p < 0.05$ ) between the  $\epsilon$  in our strain (CS-20) and the two strains grown by Sutton et al. (2013) (Table 2).

Mean values for  $\epsilon$  varied between the Fe-replete and Fe-limited conditions for the two Southern Ocean diatoms (Table 2). While there was some variability in the values of  $\epsilon$  for *E. Antarctica*, there was a significant difference in  $\epsilon$  ( $p = 0.04$ ) between Fe-replete and Fe-limited conditions, with mean  $\epsilon$  values being more negative for Fe-limited cultures (Fe-limited,  $\epsilon = -1.57 \pm 0.50$  ‰; Fe-replete,  $\epsilon = -1.40 \pm 0.41$  ‰) (Table 1). Mean  $\epsilon$  values were also more negative for *P. inermis* cultured under Fe-limited conditions (Fe-limited,  $\epsilon = -1.38 \pm 0.27$  ‰; Fe-replete,  $\epsilon = -1.11 \pm 0.15$  ‰). Both Fe-replete and Fe-limited datasets for *P. inermis* exhibited a significant difference at the 90% confidence interval ( $p = 0.08$ ), and removing outliers from both Fe-replete and Fe-limited data sets for *P. inermis* makes the difference more significant ( $p = 0.04$ ).

# DISCUSSION

This is the first study to specifically investigate the effects of Fe-limitation on Si-isotope fractionation in diatoms. Previous work has demonstrated that Fe-limitation can alter  $\text{Si(OH)}_4$  uptake kinetics, cell morphology and nutrient stoichiometry in diatoms (Hutchins and Bruland, 1998; Takeda, 1998; Brzezinski et al., 2002; Leynaert et al., 2004; Meyerink et al., 2017). Here, the processes by which Si isotopes are fractionated during diatom Si uptake and cell wall synthesis are explored and related back to mechanisms involving  $\text{Si(OH)}_4$  uptake.

## Fractionation of Si-Isotopes in Diatoms

Whilst little effect in the variability of the Si-isotope fractionation factor was observed in *T. pseudonana* in response to Fe-stress (Figure 2B), both Southern Ocean species exhibited a fractionation factor that was more negative under Fe-limitation (Figure 2A). Values for  $\epsilon$  have been observed to vary under optimal growth conditions between diatom species (Sutton et al., 2013), so it is possible that there may be an inter-species effect when it comes to environmental controls on Si-isotope fractionation in diatoms. Sutton et al. (2013) demonstrated that Si-isotope fractionation can vary by as much as 1.5 ‰ between diatom species, enough to potentially confound palaeoceanographic interpretations utilizing  $\delta^{30}\text{Si}$  from diatom opal to estimate the nutrient status of the surface ocean. In addition to interspecies effects, variations in the value for  $\epsilon$  between individual diatom strains have been observed (Sutton et al., 2013). Silicon isotope fractionation independently measured in *T. weissflogii* across three separate studies yielded  $\epsilon$  values ranging between  $-0.72 \pm 0.04$  ‰ and  $-1.5 \pm 0.1$  ‰ (De La Rocha et al., 1997; Milligan et al., 2004; Sutton et al., 2013). Similar variations have also been observed for three *T. pseudonana* clones;  $-0.61 \pm 0.21$  ‰ measured in this study and  $-0.94 \pm 0.14$  ‰ and  $-0.88 \pm 0.06$  ‰ measured for two clones cultured by Sutton et al. (2013). Sutton et al. (2013) suggest that the differences in  $\epsilon$  values for *T. weissflogii* can be attributable to the diatom being a coastal isolate rather than an open ocean isolate. There were remarkable similarities, however, in  $\epsilon$  values between the two *T. pseudonana* strains (CCMP1014 and CCCM58) cultured by Sutton et al. (2013), even though CCMP1014 is an open ocean isolate from the (North Pacific Gyre; <https://ncma.bigelow.org/>) and CCCM58 is a coastal isolate (Moriches Bay, Long island, NY; <http://www3.botany.ubc.ca/cccm/index.html>). While it is possible that inherent differences between strains as a result of the growth conditions in their endemic environment, variations culturing conditions need to be ruled out first before this hypothesis can be invoked.

## Potential Mechanisms Controlling Si Isotope Fractionation in Diatoms

Silicon-processing in diatoms is affected by Fe bioavailability (Meyerink et al., 2017) and hence can manifest to variations in the  $\delta^{30}\text{Si}$  composition of diatom silica. Understanding how diatoms fractionate Si isotopes during uptake and bio-mineralization requires a thorough investigation into how diatoms take up  $\text{Si(OH)}_4$  from the surrounding water column and use it in the formation of their cell frustules (Sutton et al., 2013; Meyerink et al., 2017). There are numerous intracellular pathways during the synthesis of biogenic silica in diatoms where fractionation of Si isotopes can potentially occur.

In diatoms,  $\text{Si(OH)}_4$  uptake from the surrounding water column is typically characterized either by diffusion or Michaelis-Menten saturation kinetics (Hildebrand, 2008; Javaheri et al., 2014). At low

ambient  $\text{Si(OH)}_4$  concentrations, uptake is mainly a saturatable process ( $\leq 10 \mu\text{mol L}^{-1}$ ), and is facilitated by Si transporters (SITs) that are localized in cell membranes (Shrestha and Hildebrand, 2015). SITs are membrane bound proteins that actively take up  $\text{Si(OH)}_4$  and transport it across the outer cell membrane to the cell cytoplasm against a concentration gradient (Hildebrand, 2008). At higher ambient  $\text{Si(OH)}_4$  concentrations ( $\geq 30 \mu\text{mol L}^{-1}$ ), diffusional uptake dominates Si acquisition with SITs playing more of a regulatory role (Thamatrakoln and Hildebrand, 2008; Shrestha and Hildebrand, 2015). Passive diffusion of  $\text{Si(OH)}_4$  appears to be proportional to the permeability of the cell membrane and the concentration gradient across the cell membrane (Hildebrand, 2008; Javaheri et al., 2014). Once past the cell membrane,  $\text{Si(OH)}_4$  is then transported intracellularly to the Si deposition vesicle (SDV) by as yet unknown transporters/compounds classified simply as “Si binding components” (Thamatrakoln and Hildebrand, 2008). Si binding components play an important role in setting the  $\text{Si(OH)}_4$  concentration gradient across the cell membrane under scenarios where diffusional uptake dominates (Thamatrakoln and Hildebrand, 2008). Active transport involving SITs likely plays an important role in facilitating the transport of Si from the cell cytoplasm into the SDV, as concentration gradients across the intracellular membrane separating the SDV from the cell cytoplasm are extremely high (Hildebrand, 2008). A new cell wall is created when the SDV is exocytosed at the M (mitosis) stage of the cell cycle. Cell wall formation during this stage is facilitated by silafins and long chain polyamines, which act as a “template” on to which the new cell wall is precipitated (Mock et al., 2008).

Fractionation of Si isotopes can potentially occur along any of these pathways. Milligan et al. (2004) explored where isotopic discrimination takes place within the cell by conducting a number of experiments where they varied the efflux:influx ratio of  $\text{Si(OH)}_4$  into and out of the cell. They suggested that fractionation of Si isotopes occurs during the membrane transport step and not during Si polymerization, as Si isotope fractionation should scale linearly with the efflux:influx ratio. In addition, the relatively small Si isotope effect may also be evidence of discrimination at the transport level, as this does not necessitate the breaking or forming of chemical bonds (Milligan et al., 2004). If this is the case, fractionation of Si isotopes occurs either at the membrane/seawater interface, as  $\text{Si(OH)}_4$  is taken up from the water column and transported to the cell cytoplasm, or, as Si is transported from the cell cytoplasm into the Silicon deposition vesicle.

## Effects of Fe-Limitation on Si-Isotope Fractionation in Diatoms

Sutton et al. (2013) observed an inter-specific variation in mean  $\epsilon$  values in Southern Ocean diatom species based on mono-culture *in-vitro* incubations. They argue that variability in diatom community composition could partly explain the observed variability in Southern Ocean Si-isotope fractionation factors. It is possible that variations in the Fe-status of certain regions in the Southern Ocean may contribute to variations in the apparent Si isotope fractionation factor. For example, Si isotope fractionation factors of diatom communities can potentially vary as a result of certain diatoms adapted to low Fe-conditions out competing other diatoms under Fe-limiting conditions. This may alter the  $\delta^{30}\text{Si}_{\text{DSi}}$  composition of surface waters. While this scenario is hypothetical, it may contribute to some of the variability in the observed relationship between the mixed layer mean apparent fractionation factor ( $\Delta^{30}\text{Si} = \delta^{30}\text{Si}_{\text{DSi}} - \delta^{30}\text{Si}_{\text{BSi}}$ ) and  $\text{Si(OH)}_4$  concentration in the Southern Ocean and the seasonal variations in Si uptake:dissolution (Varela et al., 2004; Cardinal et al., 2007; Fripiat et al., 2012).

Silicon metabolism in diatoms is particularly sensitive to variations in Fe-supply and as such,

variations in  $\epsilon$  can potentially be dependent on Fe-induced physiological variations within the cell. A notable result from our study was the relative response in the Si isotope fractionation factor ( $\epsilon$ ) of *T. pseudonana* under Fe-limitation compared to *P. inermis* and *E. Antarctica*. *T. pseudonana* exhibited no variation in  $\epsilon$  in response to Fe-limitation, and maintained a mean  $\epsilon$  value of  $-0.61 \pm 0.21$  ‰ across all Fe' concentrations. In contrast, we observed a negative response in Si isotope fractionation as a result of increased Fe-limitation in both Southern Ocean species (Figure 2). The reason behind this difference could lie in how Si is metabolized by Southern Ocean diatoms under Fe-stress.

Kinetic uptake experiments show diatoms decrease their  $\text{Si}(\text{OH})_4$  uptake rate under Fe-limitation (Franck et al., 2000; Leynaert et al., 2004; Meyerink et al., 2017). This is generally manifested by a reduction in the maximal  $\text{Si}(\text{OH})_4$  uptake rate ( $V_{\text{Si-max}}$ ) and half saturation constant ( $K_{\text{Si}}$ ). In addition, diatoms grown under Fe-limiting conditions generally exhibit reductions in their growth rate, and variations in their cell morphology. A recent study by Meyerink et al. (2017) investigated the effects of Fe availability on the  $\text{Si}(\text{OH})_4$  uptake kinetics of two Southern Ocean diatoms (*E. Antarctica* and *P. inermis*) and a coastal isolate (*T. pseudonana*). An interesting result from the study shows that when  $V_{\text{Si-max}}$  is normalized to cell surface area, it exhibits a linear relationship with cell growth rate. This relationship is independent of any variations in cell morphology or species. It is likely that this relationship can be explained by the fact that silicon uptake in the diatoms was under diffusion control, as they were acclimatized under high Si conditions. Under diffusion controlled uptake, the  $V_{\text{Si-max}}$  values reflect the realized  $\text{Si}(\text{OH})_4$  uptake rates in culture which at steady state cannot exceed cellular demands for  $\text{Si}(\text{OH})_4$  (Thamatrakoln and Hildebrand, 2008). In contrast, variations in  $K_{\text{Si}}$  in response to Fe availability exhibited no relationship with other cell parameters, however it was noticeably higher in value in the Southern Ocean species than the  $K_{\text{Si}}$  value for *T. pseudonana*. This is likely because the Southern Ocean diatoms are well adapted to growing under high Si conditions.

Diatoms with a high  $K_{\text{Si}}$  for  $\text{Si}(\text{OH})_4$  such as *E. Antarctica* and *P. inermis* ( $\geq 10 \mu\text{mol L}^{-1}$ ) (Meyerink et al., 2017) could possibly fractionate Si-isotopes differently to diatoms with a relatively low  $K_{\text{Si}}$  such as *T. pseudonana* because of their likely dependence on diffusional uptake of  $\text{Si}(\text{OH})_4$  at concentrations greater than  $30 \mu\text{mol L}^{-1}$  (Thamatrakoln and Hildebrand, 2008). Under Fe-limitation, diatoms decrease their cellular growth rate, which results in a subsequent decrease in their maximal  $\text{Si}(\text{OH})_4$  uptake rate ( $V_{\text{Si-max}}$ ) (Franck et al., 2000; Leynaert et al., 2004; Meyerink et al., 2017). This may result in a decrease in a diatoms specific affinity for  $\text{Si}(\text{OH})_4$  that can be maintained by a decrease in the  $K_{\text{Si}}$  (Franck et al., 2000; Leynaert et al., 2004; Meyerink et al., 2017). Previous studies suggest that diatoms maintain their affinity by altering their cell size (Leynaert et al., 2004); however, *E. Antarctica* exhibits a 2-fold decrease in  $K_{\text{Si}}$  when Fe-limited, which is concomitant with an increase in cell-size (Meyerink et al., 2017). It is therefore more likely that diatoms maintain their affinity for  $\text{Si}(\text{OH})_4$  by adjusting the point where diffusive transport takes over from active transport. Active transport persists at  $\text{Si}(\text{OH})_4$  concentrations greater than  $30 \mu\text{mol L}^{-1}$  under Fe-limitation, and as a result, could possibly induce a decrease in the diatoms Si-isotope fractionation factor (Shrestha and Hildebrand, 2015). If this is correct, why do *E. Antarctica* and *P. inermis* exhibit a more negative response in  $\epsilon$  when compared to *T. pseudonana*? It is possible that different genera of diatoms switch from active to diffusive transport at different  $\text{Si}(\text{OH})_4$  concentrations. While *T. pseudonana* does this at  $\sim 30 \mu\text{mol L}^{-1}$  under Fe-replete conditions (Shrestha and Hildebrand, 2015), this value could be

higher for Southern Ocean diatoms. When diatoms approached Fe-limiting conditions, such as in this study, *T. pseudonana* possibly remained under the threshold where active transport takes place, while *E. Antarctica* and *P. inermis* did not. If this is the case, then Si-isotope signatures may potentially be subject to the synergistic effects of species diversity and resource limitation.

## CONCLUSIONS

This is the first culture study to investigate the effects of Fe-limitation on Si-isotope fractionation in diatoms. Whilst any effects arising from Fe-limitation on the value of  $\epsilon$  were not evident in *T. pseudonana*, we observed that both Southern Ocean diatoms under Fe-limitation exhibit mean  $\epsilon$  values that are 0.19–0.27‰ (within error) more negative compared to Fe-replete values. While this variation is likely not enough to have any significant effect on interpretations involving  $\delta^{30}\text{Si}$  in diatomaceous opal or sea surface  $\text{Si}(\text{OH})_4/\text{BSi}$ , the finding that the value for  $\epsilon$  in the Southern Ocean species was prone to changes in the physico-chemical environment compared to that of the coastal species highlights the need to improve our understanding of how diatoms fractionate Si-isotopes during Si-uptake and frustule formation, and thus, warrants further investigation into the biochemical pathways in diatoms where Si-isotope fractionation can potentially occur.

## AUTHOR CONTRIBUTIONS

SM and ME conceived of the research. SM undertook the experiments and SM and ME interpreted the results with contributions from WM and RS. SM wrote the manuscript with contributions from ME, WM, and RS.

## ACKNOWLEDGMENTS

The Australian Research Council (DP130100679) and the Australian Antarctic Division (AAD Project 3120) are acknowledged for financial support of this work. The Authors would also like to thank two reviewers for their helpful comments.

## REFERENCES

- Beucher, C. P., Brzezinski, M. A., and Crosta, X. (2007). Silicic acid dynamics in the glacial sub-Antarctic: implications for the silicic acid leakage hypothesis. *Global Biogeochem. Cycles* 21:GB3015. doi: 10.1029/2006GB002746
- Beucher, C. P., Brzezinski, M. A., and Jones, J. L. (2011). Mechanisms controlling silicon isotope distribution in the Eastern Equatorial Pacific. *Geochim. Cosmochim. Acta* 75, 4286–4294. doi: 10.1016/j.gca.2011.05.024
- Boutorh, J., Moriceau, B., Gallinari, M., Ragueneau, O., and Bucciarelli, E. (2016). Effect of trace metal-limited growth on the postmortem dissolution of the marine diatom *Pseudo-nitzschia delicatissima*. *Global Biogeochem. Cycles* 30, 57–69. doi: 10.1002/2015GB005088
- Brzezinski, M. A., Pride, C. J., Franck, V. M., Sigman, D. M., Sarmiento, J. L., Matsumoto, K., et al. (2002). A switch from  $\text{Si}(\text{OH})_4$  to  $\text{NO}_3^-$  depletion in the glacial Southern Ocean. *Geophys. Res. Lett.* 29, 5-1–5-4. doi: 10.1029/2001gl014349

- Cardinal, D., Savoye, N., Trull, T. W., Dehairs, F., Kopczynska, E. E., Fripiat, F., et al. (2007). Silicon isotopes in spring Southern Ocean diatoms: large zonal changes despite homogeneity among size fractions. *Mar. Chem.* 106, 46–62. doi: 10.1016/j.marchem.2006.04.006
- Clayton, T. D., and Byrne, R. H. (1993). Spectrophotometric seawater pH measurements: total hydrogen ion concentration scale calibration of m-cresol purple and at-sea results. *Deep Sea Res. Pt I* 40, 2115–2129. doi: 10.1016/0967-0637(93)90048-8
- Criss, R. E., and Criss, R. (1999). *Principles of Stable Isotope Distribution*. New York, NY: Oxford University Press.
- De La Rocha, C., Brzezinski, M., DeNiro, M., and Shemeshk, A. (1998). Silicon-isotope composition of diatoms as an indicator of past oceanic change. *Phys. Rev. Lett.* 77, 2041–2044.
- De La Rocha, C. L., Brzezinski, M. A., and DeNiro, M. J. (1997). Fractionation of silicon isotopes by marine diatoms during biogenic silica formation. *Geochim. Cosmochim. Acta* 61, 5051–5056. doi: 10.1016/S0016-7037(97)00300-1
- Ellwood, M. J., Boyd, P. W., and Sutton, P. (2008). Winter-time dissolved iron and nutrient distributions in the Subantarctic zone from 40–52S; 155–160E. *Geophys. Res. Lett.* 35:L11604. doi: 10.1029/2008gl033699
- Ellwood, M. J., Wille, M., and Maher, W. (2010). Glacial silicic acid concentrations in the Southern Ocean. *Science* 330, 1088–1091. doi: 10.1126/science.1194614
- Franck, V. M., Brzezinski, M. A., Coale, K. H., and Nelson, D. M. (2000). Iron and silicic acid concentrations regulate Si uptake north and south of the polar frontal zone in the Pacific sector of the Southern Ocean. *Deep Sea Res. Pt II* 47, 3315–3338. doi: 10.1016/S0967-0645(00)00070-9
- Fripiat, F., Cavagna, A.-J., Dehairs, F., Brauwere, A. D., André, L., and Cardinal, D. (2012). Processes controlling the Si-isotope composition in the Southern Ocean and application for paleoceanography. *Biogeosciences* 9, 2443–2457. doi: 10.5194/bg-9-2443-2012
- Fripiat, F., Cavagna, A.-J., Dehairs, F., Speich, S., André, L., and Cardinal, D. (2011). Silicon pool dynamics and biogenic silica export in the Southern Ocean inferred from Si-isotopes. *Ocean Sci.* 7, 533–547. doi: 10.5194/os-7-533-2011
- Hildebrand, M. (2008). Diatoms, biomineralization processes, and genomics. *Chem. Rev.* 108, 4855–4874. doi: 10.1021/cr078253z
- Hoffmann, L., Peeken, I., and Lochte, K. (2008). Iron, silicate, and light co-limitation of three Southern Ocean diatom species. *Polar Biol.* 31, 1067–1080. doi: 10.1007/s00300-008-0448-6
- Hutchins, D. A., and Bruland, K. W. (1998). Iron-limited diatom growth and Si:N uptake ratios in a coastal upwelling regime. *Nature* 393, 561–564. doi: 10.1038/31203
- Javaheri, N., Dries, R., and Kaandorp, J. (2014). Understanding the sub-cellular dynamics of silicon transportation and synthesis in diatoms using population-level data and computational optimization. *PLoS Comput. Biol.* 10:e1003687. doi: 10.1371/journal.pcbi.1003687
- Kemp, A. E. S., Pike, J., Pearce, R. B., and Lange, C. B. (2000). The “Fall dump” – a new perspective on the role of a “shade flora” in the annual cycle of diatom production and export flux. *Deep Sea Res. Pt II* 47, 2129–2154. doi: 10.1016/S0967-0645(00)00019-9
- Leynaert, A., Bucciarelli, E., Claquin, P., Dugdale, R. C., Martin-Jezequel, V., Pondaven, P., et al. (2004). Effect of iron deficiency on diatom cell size and silicic acid uptake kinetics. *Limnol. Oceanogr.* 49, 1134–1143. doi: 10.4319/lo.2004.49.4.1134
- Maldonado, M. T., Strzepek, R. F., Sander, S., and Boyd, P. W. (2005). Acquisition of iron bound to strong organic complexes, with different Fe binding groups and photochemical reactivities, by plankton communities in Fe-limited subantarctic waters. *Global Biogeochem. Cycles* 19:GB4S23. doi: 10.1029/2005GB002481
- Marchetti, A., and Cassar, N. (2009). Diatom elemental and morphological changes in response to iron limitation: a brief review with potential paleoceanographic applications. *Geobiology* 7, 419–431. doi: 10.1111/j.1472-4669.2009.00207.x
- Martinez-Garcia, A., Rosell-Mele, A., Jaccard, S. L., Geibert, W., Sigman, D. M., and Haug, G. H. (2011). Southern Ocean dust-climate coupling over the past four million years. *Nature* 476, 312–315. doi: 10.1038/nature10310
- Matsumoto, K., Chase, Z., and Kohfeld, K. (2014). Different mechanisms of silicic acid leakage and their biogeochemical consequences. *Paleoceanography* 29, 238–254. doi: 10.1002/2013PA002588
- Matsumoto, K., Sarmiento, J. L., and Brzezinski, M. A. (2002). Silicic acid leakage from the Southern Ocean: a possible explanation for glacial atmospheric pCO<sub>2</sub>. *Global Biogeochem. Cycles* 16, 5–1. doi: 10.1029/2001GB001442
- McManus, J., Hammond, D. E., Berelson, W. M., Kilgore, T. E., Demaster, D. J., Ragueneau, O. G., et al. (1995). Early diagenesis of biogenic opal: dissolution rates, kinetics, and paleoceanographic implications. *Deep Sea Res. Pt II* 42, 871–903. doi: 10.1016/0967-0645(95)00035-O
- Meyerink, S. W., Ellwood, M. J., Maher, W. A., Price, G. D., and Strzepek, R. F. (2017). Effects of iron limitation on silicon uptake kinetics and elemental stoichiometry in two Southern Ocean diatoms, *Eucampia antarctica* and *Proboscia inermis*, and the temperate diatom *Thalassiosira pseudonana*. *Limnol. Oceanogr.* doi: 10.1002/lno.10578. [Epub ahead of print].
- Milligan, A. J., Varela, D. E., Brzezinski, M. A., and Morel, F. M. M. (2004). Dynamics of silicon metabolism and silicon isotopic discrimination in a marine diatom as a function of pCO<sub>2</sub>. *Limnol. Oceanogr.* 49, 322–329. doi: 10.4319/lo.2004.49.2.0322
- Mock, T., Samanta, M. P., Iverson, V., Berthiaume, C., Robison, M., Holtermann, K., et al. (2008). Whole-genome expression profiling of the marine diatom *Thalassiosira pseudonana* identifies genes involved in silicon bioprocesses. *Proc. Nat. Acad. Sci. U.S.A.* 105, 1579–1584. doi: 10.1073/pnas.0707946105

- Nelson, D. M., Treguer, P., Brzezinski, M. A., Leynaert, A., and QuÉguiner, B. (1995). Production and dissolution of biogenic silica in the ocean: revised global estimates, comparison with regional data and relationship to biogenic sedimentation. *Global Biogeochem. Cycles* 9, 359–372. doi: 10.1029/95GB01070
- Pichevin, L. E., Reynolds, B. C., Ganeshram, R. S., Cacho, I., Pena, L., Keefe, K., et al. (2009). Enhanced carbon pump inferred from relaxation of nutrient limitation in the glacial ocean. *Nature* 459, 1114–1117. doi: 10.1038/nature08101
- Price, N. M., Harrison, G. I., Hering, J. G., Hudson, R. J., Nirel, P. M., Palenik, B., et al. (1988). Preparation and chemistry of the artificial algal culture medium Aquil. *Biol. Oceanogr.* 6, 443–461.
- Ragueneau, O., Treguer, P., Leynaert, A., Anderson, R. F., Brzezinski, M. A., DeMaster, D. J., et al. (2000). A review of the Si cycle in the modern ocean: recent progress and missing gaps in the application of biogenic opal as a paleoproductivity proxy. *Glob. Planet. Change* 26, 317–365. doi: 10.1016/S0921-8181(00)00052-7
- Reynolds, B. C., Aggarwal, J., André, L., Baxter, D., Beucher, C., Brzezinski, M. A., et al. (2007). An inter-laboratory comparison of Si isotope reference materials. *J. Anal. Atom. Spectrom.* 22, 561–568. doi: 10.1039/B616755A
- Roca-Martí, M., Puigcorbé, V., Iversen, M. H., van der Loeff, M. R., Klaas, C., Cheah, W., et al. (2017). High Particulate organic carbon export during the decline of a vast diatom bloom in the Atlantic sector of the Southern Ocean. *Deep-Sea Res. Pt. II* 138, 102–115. doi: 10.1016/j.dsr2.2015.12.007
- Rousseau, J., Ellwood, M. J., Bostock, H., and Neil, H. (2016). Estimates of late Quaternary mode and intermediate water silicic acid concentration in the Pacific Southern Ocean. *Earth Planet. Sci. Lett.* 439, 101–108. doi: 10.1016/j.epsl.2016.01.023
- Sackett, O., Petrou, K., Reedy, B., De Grazia, A., Hill, R., Doblin, M., et al. (2013). Phenotypic plasticity of southern ocean diatoms: key to success in the sea ice habitat? *PLoS ONE* 8:e81185. doi: 10.1371/journal.pone.0081185
- Shrestha, R. P., and Hildebrand, M. (2015). Evidence for a regulatory role of diatom silicon transporters in cellular silicon responses. *Eukaryot. Cell* 14, 29–40. doi: 10.1128/EC.00209-14
- Smetacek, V. (1999). Diatoms and the ocean carbon cycle. *Protist* 150, 25–32. doi: 10.1016/S1434-4610(99)70006-4
- Strickland, J. D. H., and Parsons, T. R. (1965). *A Manual of Sea Water Analysis*. Ottawa, ON: Fisheries Research Board of Canada.
- Strzepek, R. F., Hunter, K. A., Frew, R. D., Harrison, P. J., and Boyd, P. W. (2012). Iron-light interactions differ in Southern Ocean phytoplankton. *Limnol. Oceanogr.* 57, 1182–1200. doi: 10.4319/lo.2012.57.4.1182
- Strzepek, R. F., Maldonado, M. T., Hunter, K. A., Frew, R. D., and Boyd, P. W. (2011). Adaptive strategies by Southern Ocean phytoplankton to lessen iron limitation: Uptake of organically complexed iron and reduced cellular iron requirements. *Limnol. Oceanogr.* 56, 1983–2002. doi: 10.4319/lo.2011.56.6.1983
- Sunda, W., and Huntsman, S. (2003). Effect of pH, light, and temperature on Fe-EDTA chelation and Fe hydrolysis in seawater. *Mar. Chem.* 84, 35–47. doi: 10.1016/S0304-4203(03)00101-4
- Sunda, W. G., and Huntsman, S. A. (1997). Interrelated influence of iron, light and cell size on marine phytoplankton growth. *Nature* 390, 389–392. doi: 10.1038/37093
- Sutton, J. N., Varela, D. E., Brzezinski, M. A., and Beucher, C. P. (2013). Species-dependent silicon isotope fractionation by marine diatoms. *Geochim. Cosmochim. Acta* 104, 300–309. doi: 10.1016/j.gca.2012.10.057
- Takeda, S. (1998). Influence of iron availability on nutrient consumption ratio of diatoms in oceanic waters. *Nature* 393, 774–777. doi: 10.1038/31674
- Thamatrakoln, K., and Hildebrand, M. (2008). Silicon uptake in diatoms revisited: a model for saturable and nonsaturable uptake kinetics and the role of silicon transporters. *Plant Physiol.* 146, 1397–1407. doi: 10.1104/pp.107.107094
- Tréguer, P., Nelson, D. M., Van Bennekom, A. J., DeMaster, D. J., Leynaert, A., and Queguiner, B. (1995). The silica balance in the world ocean: a reestimate. *Science* 268:375. doi: 10.1126/science.268.5209.375
- Tréguer, P. J., and De La Rocha, C. L. (2013). The world ocean silica cycle. *Ann. Rev. Mar. Sci.* 5, 477–501. doi: 10.1146/annurev-marine-121211-172346
- Varela, D. E., Pride, C. J., and Brzezinski, M. A. (2004). Biological fractionation of silicon isotopes in Southern Ocean surface waters. *Global Biogeochem. Cycles* 18. doi: 10.1029/2003GB002140
- Wille, M., Sutton, J., Ellwood, M. J., Sambridge, M., Maher, W., Eggins, S., et al. (2010). Silicon isotopic fractionation in marine sponges: A new model for understanding silicon isotopic variations in sponges. *Earth Planet. Sci. Lett.* 292, 281–289. doi: 10.1016/j.epsl.2010.01.036
- Yao, W., Liu, X., and Byrne, R. H. (2007). Impurities in indicators used for spectrophotometric seawater pH measurements: assessment and remedies. *Mar. Chem.* 107, 167–172. doi: 10.1016/j.marchem.2007.06.012

**Conflict of Interest Statement:** The authors declare that the research was conducted in the absence of any commercial or financial relationships that could be construed as a potential conflict of interest.

Copyright © 2017 Meyerink, Ellwood, Maher and Strzepek. This is an open-access article

*distributed under the terms of the Creative Commons Attribution License (CC BY). The use, distribution or reproduction in other forums is permitted, provided the original author(s) or licensor are credited and that the original publication in this journal is cited, in accordance with accepted academic practice. No use, distribution or reproduction is permitted which does not comply with these terms.*